Nanoscale

RSC Publishing

COMMUNICATION

View Article Online
View Journal | View Issue

Cite this: *Nanoscale*, 2013, **5**, 8488

Received 27th May 2013
Accepted 12th July 2013

DOI: 10.1039/c3nr02742b

www.rsc.org/nanoscale

Development of stretchable membrane based nanofilters using patterned arrays of vertically grown carbon nanotubes†

Hao Wang,[ab] Zhuolin Xiang,[a] Chih-Fan Hu,[c] Aakanksha Pant,[b] Weileun Fang,[c] Sylvie Alonso,[d] Giorgia Pastorin*[b] and Chengkuo Lee*[a]

A unique process which utilizes membrane based vertically grown carbon nanotubes (CNTs) as nanofilters for a mass transport study is presented here. By using ions, ss-DNA and haemagglutinin as testing molecules of different dimensions, the mass transport function of the CNT membrane is investigated under pressure difference and/or electric field.

Nanometer scale filters of high chemical selectivity and high flux are strongly desired for chemical separation,[1–6] drug delivery[7–10] and wastewater remediation.[11] To investigate the effects of target molecules *versus* pore size and force interactions between target molecules and surface state of pores, many approaches regarding the fabrication of nano-scale filters of pore sizes ranging from 1 to 10 nm have been characterized, which include functionalized polymer affinity membranes,[12] block copolymers,[13] mesoporous macromolecular architectures[13] and hollow carbon nanotubes (CNTs).[1–3,5,6,13–24] Among these, CNTs are a very promising material. Vertically aligned CNT forests grown from macro- or micro-patterned catalyst layers have been reported.[25,26] When compared with other nanofabrication technologies,[27] the CNT growth techniques are easier, cheaper and more suitable for mass fabrication. On the other hand, investigation on mass transport through CNTs has been an interesting topic as well.[1,28–46] Most of these studies just focus on the study of mass transport by applying an electric field since their devices are too fragile to withstand any pressure. Mass transport through CNTs by applying pressure remains an unexplored topic. More importantly, none of these reported devices yet use patterned CNT forests which is also highly desired for further integration with other microfluidics to make a complicated device with advanced functions. To overcome these two advantages and explore the application of CNT nanofilters, a unique process is proposed to fabricate membrane based CNT nanofilters using patterned CNT bundles in this paper. This membrane based CNT nanofilters can withstand high pressure. This attractive feature has an impact on the current nano-scale filters.

Our devices enable us to study the mass transport and filter function at high pressure. This high pressure environment is preferred in various practical applications for nanofilters. Characterization of ion transport by both pressure and electric field is carried out to ensure the functionality of the CNT membranes. Two molecules, ss-DNA and haemagglutinin, of different dimensions are used in permeability tests to show that the CNT membranes fabricated could be deployed as nanofilters which enable selective drug delivery by size exclusion. Finally, diffusion of bacteria is investigated to prove the nanofilter function which can successfully block bacteria and is preferred for drug purification and separation.

Scheme 1 shows the experimental steps for the fabrication of membrane based nanofilters shown in Fig. 1 using patterned CNT bundles. A substrate with arrays of vertically aligned CNT patterns (Fig. 2(a)) is first reinforced by CVD grown parylene (Scheme 1, step 1) so that parylene molecules are infiltrated into the intertube space (Fig. 2(b)). The parylene layer together with patterned CNT arrays is then peeled off from the substrate and the catalyst layer on the backside is etched off by oxygen plasma (Scheme 1, step 2). The backside catalyst layer is shown in Fig. 2(c). The catalyst layer is etched away by oxygen plasma (Fig. 2(d)). The released parylene layer is then attached to a prebaked SU-8 substrate. The Su-8 substrate is baked and cooled to achieve bonding with parylene (Scheme 1, step 3). Vertical microfluidic channels under CNT bundles shown in

[a]*Electrical and Computer Engineering, National University of Singapore, Engineering Drive 3, 117576, Singapore. E-mail: elelc@nus.edu.sg*

[b]*Department of Pharmacy, National University of Singapore, 18 Science Drive 4, 117543, Singapore. E-mail: phapg@nus.edu.sg*

[c]*Institute of NanoEngineering and MicroSystems/Department of Power Mechanical Engineering, National Tsing Hua University, 101, Section 2, Kuang-Fu Road, Hsinchu, Taiwan, 30013, R. O. C. E-mail: fang@pme.nthu.edu.tw*

[d]*Department of Microbiology, Immunology Programme, National University of Singapore, 10 Kent Ridge Crescent, 119260, Singapore. E-mail: micas@nus.edu.sg*

† Electronic supplementary information (ESI) available: Preparation of ss-DNA and BPSM and detailed fabrication process for CNT nanofilters. See DOI: 10.1039/c3nr02742b

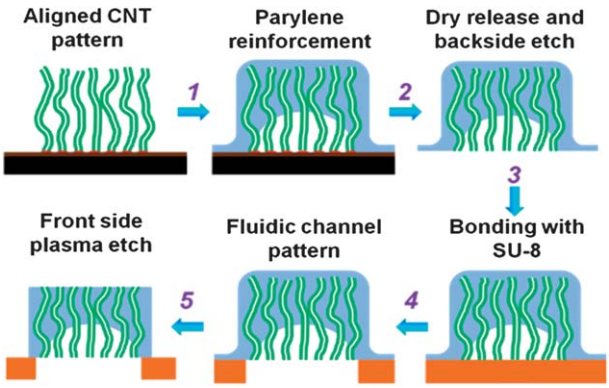

Scheme 1 Schematic representation of the experimental steps showing the fabrication of membrane based nanofilters.

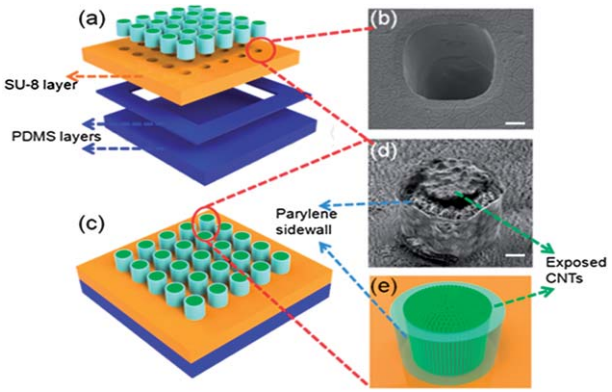

Fig. 1 (a) 3D schematic drawing of the detailed layer structure of the devices. (b) SEM picture taken from the back side of the SU-8 layer showing a hole under a CNT bundle on the SU-8 layer. (c) 3D schematic drawing of the device. (d) SEM picture of the CNT bundles with top end open; (e) 3D schematic drawing of the CNT bundle with top end open. The scale bar for (b) and (d) is 10 μm.

Fig. 1(b) are patterned by standard lithography (Scheme 1, step 4). The bottom sides of the CNT bundles are open. The top sides of the CNT bundles are opened by oxygen plasma etching (Scheme 1, step 5). Fig. 1(d) shows the CNT bundles with top open. Fig. 1(e) shows the 3D schematic drawing of the open CNT bundle for a better understanding. The whole parylene layer is etched off since there was no mask in the etching process. The parylene sidewall remains due to the anisotropic property of plasma etching. These parylene sidewalls provide bonding which makes the CNT bundles fix onto the SU-8 substrate. Two PDMS layers are further bonded at the bottom of the device for tubing and tests (Fig. 1(a) and (b)). The detailed steps are depicted in Fig. S1 of the ESI.†

The bonding strength between parylene and SU-8 is very strong. The detachment between parylene and substrate[20] will not occur here. Because we use CNT bundles of small patterns instead of whole CNT forests of large area, the CNT forests will not break by applying pressure. These two differences make our device withstand high pressure.

The mass transport of ions and biomolecules of nanofilter samples of different dimensions is measured by applying an electric field and pressure based on the test setup shown in Fig. 3(a).

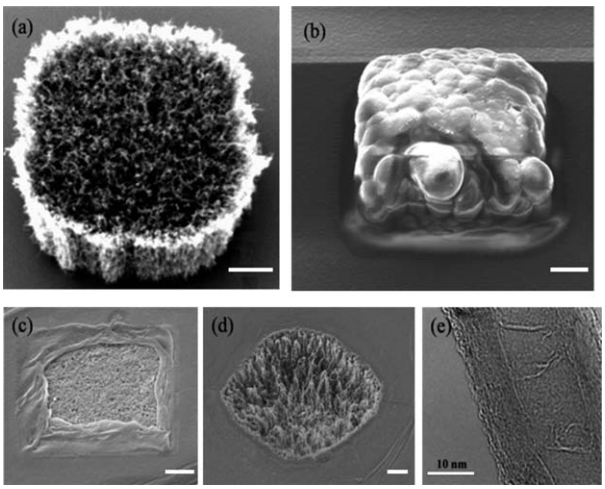

Fig. 2 (a) An individual CNT bundle grows from the catalyst layer, the diameter of the CNT bundle is 50 μm, and the height of the CNT bundle is 50 μm; (b) an individual CNT bundle reinforced by parylene; the thickness of the parylene layer is 10 μm; (c) the catalyst layer seals the bottom of the CNT bundle; (d) the catalyst layer is etched by oxygen plasma; (e) TEM picture showing the inner diameter of the CNTs as 10 nm; the scale bar for (a) to (d) is 10 μm.

A Ti electrode penetrated the PDMS layer and connected the solution inside the PDMS chamber. Bias could be applied *via* this electrode. A test solution of a very small volume was pre-loaded in the device chamber and part of the tube. This preloading is necessary to get rid of the air in the device chamber and make the solution in contact with the surface of CNT bundles. The tube connected the device with a syringe and a pressure sensor. The syringe could be driven by a syringe pump to give air pressure and the air pressure is calibrated using the pressure sensor.

Based on our observation, the CNT nanofilters are able to sustain under a pressure level of 40 kPa, but for some samples, leakage between the interface of PDMS and SU-8 was detected at a pressure level higher than 25 kPa. Thus, the pressure level was limited within 25 kPa in our experiments. The device was loaded in the beaker. The liquid surface in the beaker should be kept lower than the exposed part of the electrode inserted in PDMS. This was to avoid the two electrodes being shorted by the solution connection. Another Ti electrode was immersed into the solution in the beaker.

The two electrodes were connected to a semiconductor characterization system (KEITHLEY 4200) which could apply bias and measure the current simultaneously. The resultant solution was sampled from the solution inside the beaker.

For the study of driving ions by an electric field, NaCl solution was loaded in both the beaker and the tube. The solution volume in the beaker was 60 ml and in the tube it was about 0.2 ml. A bias of 5 V was applied between the two Ti electrodes for 160 min. The electrode in the beaker was grounded and the electrode in the tube was positively biased. No air pressure is applied. No obvious electrolysis of water is observed. Two concentrations of NaCl solution, 1 mol L^{-1} and 0.1 mol L^{-1}, were employed to study the relationship between the ion concentration and the ionic current. The experiments were

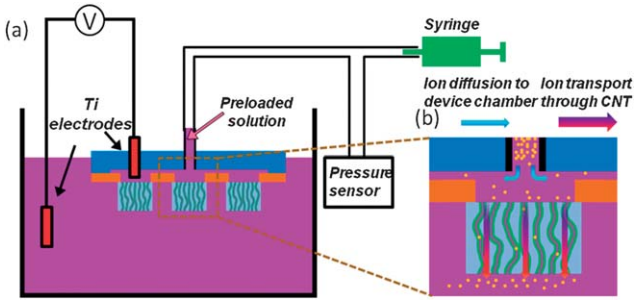

Fig. 3 (a) Test setup for applying an electric field and pressure; (b) schematic drawing of the ion diffusion and ion depletion in the device chamber.

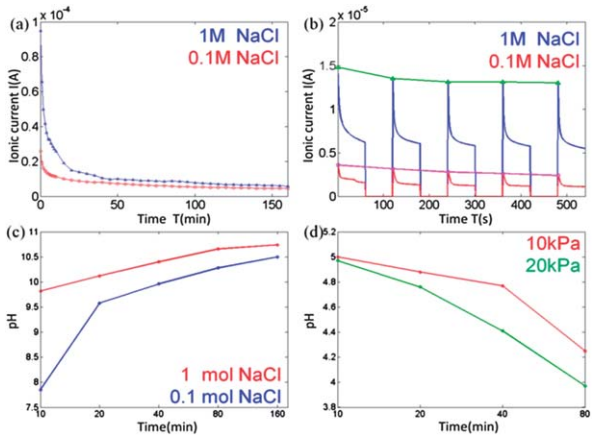

Fig. 4 (a) The ionic current through the CNT membranes as a function of time in different NaCl concentrations; (b) the ionic current as a function of time under square wave bias in different NaCl concentrations. The green line and pink line indicate the difference between peak values of the ionic current. (c) The pH value of the NaCl solution with different concentrations as a function of time; (d) the pH value of the HCl solution under different driving pressures as a function of time.

carried out at room temperature (~26 °C). The solution in the beaker was sampled for pH measurement at 10, 20, 40, 80 and 160 min. The change of ionic current was recorded as shown in Fig. 4(a). The ionic current quickly dropped down as a function of time. The peak values of the ionic current of NaCl concentration 0.1 mol L^{-1} and 1 mol L^{-1} were 9.5×10^{-5} A and 2.4×10^{-5} A, respectively. The large peak value difference suggests that the main transport mechanism under an electric field is through electrophoresis.[23] The drop of the ionic current may be due to two possible reasons. First, the change of pH value altered the property of the CNTs' inner wall surface which enhanced the interaction between ions and CNTs' inner wall surface. This pH value change was caused by electrolysis of NaCl solution. The reaction in the beaker is:

$$2NaCl + 2H_2O + 2e^- \rightarrow 2NaOH + H_2\uparrow + 2Cl^-;$$

so the solution will be alkaline and the pH value will rise. And the reaction in the tube is:

$$2NaCl + 2H_2O \rightarrow 2Na^+ + HCl + HOCl + 2e^-;$$

so the solution will be acidic and the pH value will drop. The change of the pH value is shown in Fig. 4(c). The NaCl solution of higher concentration had a higher pH value which indicates a faster reaction rate. And the difference of pH value inside the beaker and tube increased with time. However, according to Fig. 4(a), the ionic current tends to stabilize with time. So the change of the pH value should not be the reason for the drop of ionic current. It is also reported that the pH value of the solution does not significantly affect the ionic current and the conductance of CNTs.[20] The second possible reason is the depletion of the ions in the PDMS chamber. The high peak values of the ionic currents stand for fast ion transport. This fast ion transport may cause depletion which cannot be compensated by the ion diffusion from other regions. As shown in Fig. 3(b), the geometry of the device chamber connecting the CNT bundles is very limited. Maybe ions cannot efficiently diffuse from other places into this region when ions at this region quickly pass through the CNT bundles. Then the depletion of ions in the PDMS chamber causes the drop of the ionic current. We carried out an experiment to prove it. The 5 V bias was applied in a square wave mode with a duty cycle of 1 min on and 1 min off. This square wave mode bias was applied for several cycles and the recorded ionic current is shown in Fig. 4(b). The ionic current dropped when the bias was on. When the bias was not off, the solution in the device chamber was replenished with ions by diffusion from other regions. Thus, when the bias was on again, the peak value of the ionic current recovered to a certain level. But since 1 min time duration was insufficient for the recovery of ion concentration in the device chamber to its initial value, the peak value of the ionic current still had a slight drop. The green line shows the drop of peak values from about 1.5×10^{-5} A to about 1.4×10^{-5} A for 1 mol L^{-1} NaCl concentration.

For the study of driving ions by pressure, 0.2 ml of 3.7% HCl solution was preloaded in the tube. 60 ml of DI water was loaded in the beaker. Air pressures of 10 kPa and 20 kPa were applied for 80 min to study the relationship between pressure and permeability with a zero bias voltage. The solution in the beaker was sampled at 10, 20, 40 and 80 min. The pH value of solution samples was measured using a pH meter (CORNING Pinnacle, Model: 530) as shown in Fig. 4(d). The line of 20 kPa pressure shows a greater pH value drop than that of 10 kPa. At 80 min, the pH values of solution after applying 10 kPa and 20 kPa were 4.25 and 3.97, respectively. According to the definition of pH value, $pH = -\log[H^+]$; $[H^+]$ refers to the H^+ concentration.

The ratio of H^+ concentration is $[H^+]_{20\ kPa}/[H^+]_{10\ kPa} = 104.25/103.97 = 1.9$. The ratio of H^+ concentration was almost the same as the ratio of pressure level. This result suggests a linear relationship between the mass transport rate and the pressure level, which is consistent with the reported result.[20]

In the study of large molecule translocation through CNT membranes, ss-DNA and haemagglutinin were employed to study the CNT bundles' filter function. The inner diameter of the CNTs in this study is 10 nm (Fig. 2(e)). The ss-DNA, the cross-sectional dimension of which is smaller than 10 nm, was expected to pass through CNT membranes just by applying pressure. And haemagglutinin, the shape of which is like a cylinder and dimension is approximately 13.5 nm long that is

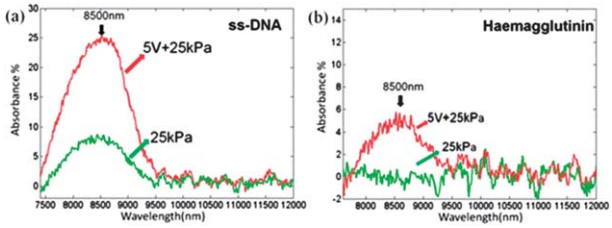

Fig. 5 (a) IR spectra of ss-DNA in the beaker after applying 25 kPa pressure and after applying both 25 kPa pressure and 5 V bias; (b) IR spectra of haemagglutinin in the beaker after applying 25 kPa pressure and after applying both 25 kPa pressure and 5 V bias.

larger than the inner diameter of the CNTs, was not expected to pass through CNT membranes by applying pressure.

A combination of pressure and electric field driven method that could drive ss-DNA through CNTs is reported.[23] In the experiment with ss-DNA, 60 ml of DI water was loaded in the beaker and a droplet of ss-DNA solution was preloaded in the tube. A pressure of 25 kPa was applied for 7 hours. The solution in the beaker was sampled after the experiment. The absorbance spectra were recorded by FTIR (Fourier transform infrared spectroscopy Cary 660-FT-IR). DI water was used as a background sample to show the absorbance in Fig. 5(a). The green line shows that ss-DNA could pass through CNT membranes just by applying pressure. The absorbance shown in Fig. 5(a) suggests that more ss-DNA could pass through CNTs by the additional electric field.

In the case of haemagglutinin under pressure driven conditions, no absorbance was observed in the spectra of samples measured at an applied pressure of 10, 15 and 20 kPa for 7 hours. Fig. 5(b) shows the measured spectrum under 25 kPa for the above samples for an additional 15 hours. Again no absorbance was observed. Then a pressure level of 25 kPa and a bias of 5 V were applied together. The measured spectrum indicates a weak absorbance as shown in Fig. 5(b). It suggests that haemagglutinin could pass through CNTs when the pressure and electric field were applied together. But the translocation rate was relatively low compared to that of ss-DNA. This is because the dimension of haemagglutinin is much larger than that of ss-DNA. The test result shows that permeability decreases with the increase of dimension of the molecule.

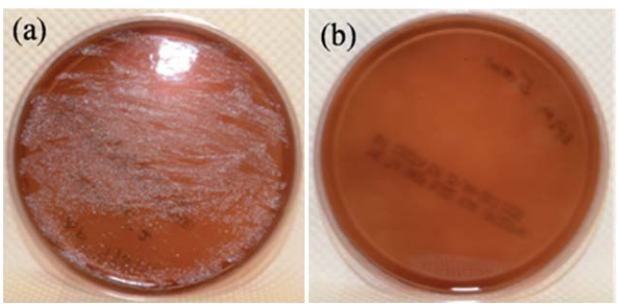

Fig. 6 (a) Result of bacterium culturing of the solution sampled from the device chamber, bacterial colonies were observed; (b) result of bacterium culturing of the solution loaded in the beaker, no bacterial colony was found.

To confirm that CNT nanofilters could block all micro-scale substances, we further tried passing bacteria through CNT nanofilters. In this experiment, PBS and BPSM (*Bordetella pertussis*, streptomycin resistant) are employed. The test setup is shown in Fig. 3(a). 0.1 ml of mixed solution was loaded in the device and PBS was loaded in the beaker. A combination of pressure and electric field driven method was used to drive the PBS through the CNT nanofilters. The pressure is 20 kPa and the electric bias is 5 V. To detect the bacteria at very low concentration, the solution should be sampled for cell culture and enrichment. To ensure that the bacteria were viable at ambient temperature during the experiment, the test was conducted for 2 hours. The solution sampled in the beaker was cultured on blood agar plates for 5 days to see whether bacteria passed through the CNT nanofilters. The solution with bacteria loaded in the device chamber was also cultured as a control group for comparison. Fig. 6(a) shows the result of bacterial culturing of the solution sampled from the device chamber. After 5 days of culturing, bacterial colonies were observed. Fig. 6(b) shows the result of bacterial culturing of the solution sampled in the beaker. No bacterial colony was found which confirms a perfect bacterium blockage.

In conclusion, we propose a new fabrication process for stretchable membrane based nanofilters using patterned arrays of vertically grown carbon nanotube bundles. The functionality is proved by pumping ions through CNT membranes either by applying pressure or electric field. A linear relationship between the mass transport rate and the driving pressure is observed. The ss-DNA could pass through the CNT membranes by applying high pressure and an additional electric field can further enhance the permeability. However, haemagglutinin the dimension of which is close to the inner diameter of the CNTs cannot pass through the CNT membranes just by applying pressure but an additional electric field could make it pass through. This proves that the permeability through CNT nanofilters is highly dependent on the molecular weight and physical dimension. Micro-scale bacteria would be totally blocked which confirms the device's high quality and reliability. The test results prove that the CNT membranes could be deployed as nanofilters working at high pressure which is not reported yet. The CNT nanofilters of patterned CNT bundles on flexible polymer materials enable further integration with other microfluidics for chemical and pharmaceutical applications. These results also indicate that the device could be used for size matching molecular sieving. Just by using the same process on CNTs of different inner diameters, the devices could be used for different kinds of chemical separation. It is also possible to involve surface functionalization to enhance the capability of chemical separation.

This work is supported by MOE: ARF-Tier 2 grant: Nanoneedle Devices for Transdermal Vaccine Delivery (WBS: 263000598112 and R-398000068112).

Notes and references

1 F. Fornasiero, J. B. In, S. Kim, H. G. Park, Y. Wang, *et al.*, O, pH-Tunable Ion Selectivity in Carbon Nanotube Pores, *Langmuir*, 2010, **26**, 14848–14853.

2 X. Sun, X. Su, J. Wu and B. J. Hinds, Electrophoretic Transport of Biomolecules through Carbon Nanotube Membranes, *Langmuir*, 2011, **27**, 3150–3156.
3 F. Fornasiero, H. G. Park, J. K. Holt, M. Stadermann, C. P. Grigoropoulos, *et al.*, Ion exclusion by sub-2 nm carbon nanotube pores, *Proc. Natl. Acad. Sci. U. S. A.*, 2008, **105**, 17250–17255.
4 L. Ge, L. Wang, A. Du, M. Hou, V. Rudolph, *et al.*, Vertically-aligned carbon nanotube membranes for hydrogen separation, *RSC Adv.*, 2012, **2**, 5329.
5 B. Hinds, Dramatic transport properties of carbon nanotube membranes for a robust protein channel mimetic platform, *Curr. Opin. Solid State Mater. Sci.*, 2012, **16**, 1–9.
6 C. H. Ahn, Y. Baek, C. Lee, S. O. Kim, S. Kim, *et al.* Carbon nanotube-based membranes: fabrication and application to desalination, *J. Ind. Eng. Chem.*, 2012, **18**, 1551–1559.
7 J. Wu, K. S. Paudel, C. Strasinger, D. Hammell, A. L. Stinchcomb, *et al.*, Programmable transdermal drug delivery of nicotine using carbon nanotube membranes, *Proc. Natl. Acad. Sci. U. S. A.*, 2010, **107**, 11698–11702.
8 S. Ilbasmis-Tamer and I. T. Degim, A feasible way to use carbon nanotubes to deliver drug molecules: transdermal application, *Expert Opin. Drug Delivery*, 2012, **9**, 991–999.
9 K. K. Jain, Advances in use of functionalized carbon nanotubes for drug design and discovery, *Expert Opin. Drug Delivery*, 2012, **7**, 1029–1037.
10 H. Dumortier, S. Lacotte, G. Pastorin, R. Marega, W. Wu, *et al.*, Functionalized Carbon Nanotubes Are Non-Cytotoxic and Preserve the Functionality of Primary Immune Cells, *Nano Lett.*, 2006, **6**, 1522–1528.
11 B. Corry, Designing Carbon Nanotube Membranes for Efficient Water Desalination, *J. Phys. Chem. B*, 2008, **112**, 1427–1434.
12 E. Klein, Affinity membranes: a 10-year review, *J. Membr. Sci.*, 2000, **179**, 1–27.
13 T. Thurn-Albrecht, R. Steiner, J. DeRouchey, C. M. Stafford, E. Huang, *et al.*, Nanoscopic Templates from Oriented Block Copolymer Films, *Adv. Mater.*, 2000, **12**, 787–791.
14 T. Asefa, M. J. MacLachlan, N. C. Coombs and G. A. Ozin, Periodic mesoporous organosilicas with organic groups inside the channel walls, *Nature*, 1999, **402**, 867–871.
15 J. Wu, K. Gerstandt, H. Zhang, J. Liu and B. J. Hinds, Electrophoretically induced aqueous flow through single-walled carbon nanotube membranes, *Nat. Nanotechnol.*, 2012, **7**, 133–139.
16 V. Lulevich, S. Kim, C. P. Grigoropoulos and A. Noy, Frictionless sliding of single-stranded DNA in a carbon nanotube pore observed by single molecule force spectroscopy, *Nano Lett.*, 2011, **11**, 1171–1176.
17 B. J. Hinds, N. Chopra, T. Rantell, R. Andrews, V. Gavalas, *et al.*, Aligned Multiwalled Carbon Nanotube Membranes, *Science*, 2004, **303**, 62–65.
18 S. Kim, J. R. Jinschek, H. Chen, D. S. Sholl and E. Marand, Scalable Fabrication of Carbon Nanotube/Polymer Nanocomposite Membranes for High Flux Gas Transport, *Nano Lett.*, 2007, **7**, 2806–11.
19 D. S. Sholl and J. K. Johnson, Making High-Flux Membranes with Carbon Nanotubes, *Science*, 2006, **312**, 1003–1004.
20 P. Krishnakumar, P. B. Tiwari, S. Staples, T. Luo, Y. Darici, *et al.*, Mass transport through vertically aligned large diameter MWCNTs embedded in parylene, *Nanotechnology*, 2012, **23**, 455101.
21 M. Whitby and N. Quirke, Fluid flow in carbon nanotubes and nanopipes, *Nat. Nanotechnol.*, 2007, **2**, 87–94.
22 D. Cao, P. Pang, J. He, T. Luo, J. H. Park, *et al.*, Electronic Sensitivity of Carbon Nanotubes to Internal Water Wetting, *ACS Nano*, 2011, **5**, 3113–3119.
23 J. Su and H. Guo, Control of Unidirectional Transport of Single-File Water Molecules through Carbon Nanotubes in an Electric Field, *ACS Nano*, 2011, **5**, 351–359.
24 J. K. Holt, H. G. Park, Y. Wang, M. Stadermann, A. B. Artyukhin, *et al.*, Fast Mass Transport Through Sub-2-Nanometer Carbon Nanotubes, *Science*, 2006, **312**, 1034–1037.
25 W. Mi, Y. S. Lin and Y. Li, Vertically aligned carbon nanotube membranes on macroporous alumina supports, *J. Membr. Sci.*, 2007, **304**, 1–7.
26 D. Varshney, V. I. Makarov, P. Saxena, J. F. Scott, B. R. Weiner, *et al.*, Genesis of diamond nanotubes from carbon nanotubes, *EPL*, 2011, **95**, 28002.
27 R. B. Schoch, J. Han and P. Renaud, Transport phenomena in nanofluidics, *Rev. Mod. Phys.*, 2008, **80**, 839.
28 M. Majumder, N. Chopra and B. J. Hinds, Mass Transport through Carbon Nanotube Membranes in Three Different Regimes: Ionic Diffusion and Gas and Liquid Flow, *ACS Nano*, 2011, **5**, 3867–3877.
29 B. Luan, D. Wang, R. Zhou, S. Harrer, H. Peng, *et al.*, Dynamics of DNA translocation in a solid-state nanopore immersed in aqueous glycerol, *Nanotechnology*, 2012, **23**, 455102.
30 Z. W. Ulissi, S. Shimizu, C. Y. Lee and M. S. Strano, Carbon Nanotubes as Molecular Conduits: Advances and Challenges for Transport through Isolated Sub-2 nm Pores, *J. Phys. Chem. Lett.*, 2011, **2**, 2892–2896.
31 W. Reisner, J. N. Pedersen and R. H. Austin, DNA confinement in nanochannels: physics and biological applications, *Rep. Prog. Phys.*, 2012, **75**, 106601.
32 D. Cai, L. Ren, H. Zhao, C. Xu, L. Zhang, *et al.*, A molecular-imprint nanosensor for ultrasensitive detection of proteins, *Nat. Nanotechnol.*, 2010, **5**, 597–601.
33 F. Fornasiero and H. Park, Nanofluidics in carbon nanotubes, *Nano Today*, 2008, **2**, 22–29.
34 C. Y. Lee, W. Choi, J.-H. Han and M. S. Strano, Coherence Resonance in a Single-Walled Carbon Nanotube Ion Channel, *Science*, 2010, **329**, 1320–1324.
35 Q. Zhou and L. Lin, Enhancing Mass Transport for Synthesizing Single-Walled Carbon Nanotubes *via* Micro Chemical Vapor Deposition, *J. Microelectromech. Syst.*, 2011, **20**, 10–12.
36 H. Liu, J. He, J. Tang, H. Liu, P. Pang, *et al.*, Translocation of Single-Stranded DNA Through Single-Walled Carbon Nanotubes, *Science*, 2010, **327**, 64–67.
37 M. Sun and Y. Gao, Electrically driven gallium movement in carbon nanotubes, *Nanotechnology*, 2012, **23**, 065704.

38 J. Zhao, J.-Q. Huang, F. Wei and J. Zhu, Mass Transportation Mechanism in Electric-Biased Carbon Nanotubes, *Nano Lett.*, 2010, **10**, 4309–4315.
39 J. He, H. Liu, P. Pang, D. Cao and S. Lindsay, Translocation events in a single-walled carbon nanotube, *J. Phys.: Condens. Matter*, 2010, **22**, 454112.
40 P. Pang, J. He, J. Park, P. Krstić and S. Lindsay, Origin of Giant Ionic Currents in Carbon Nanotube Channels, *ACSNano*, 2011, **5**, 7277–7283.
41 X. Qin, Q. Yuan, Y. Zhao, S. Xie and Z. Liu, Measurement of the Rate of Water Translocation through Carbon Nanotubes, *Nano Lett.*, 2011, **11**, 2173–2177.
42 J. K. Holt, Carbon Nanotubes and Nanofluidic Transport, *Adv. Mater.*, 2009, **21**, 3542–3550.
43 D. Mattia and Y. Gogotsi, Review: static and dynamic behavior of liquids inside carbon nanotubes, *Microfluid. Nanofluid.*, 2008, **5**, 289–305.
44 M. Whitby, L. Cagnon, M. Thanou and N. Quirke, Enhanced Fluid Flow through Nanoscale Carbon Pipes, *Nano Lett.*, 2008, **8**, 2632–2637.
45 C. Shearer, L. Velleman, F. Acosta, A. Ellis and N. Voelcker *et al.*, Water transport through nanoporous materials: Porous silicon and single walled carbon nanotubes, in *2010 International Conference on Nanoscience and Nanotechnology*, 2010, pp. 196–199.
46 H. Verweij, M. C. Schillo and J. Li, Fast Mass Transport Through Carbon Nanotube Membranes, *Small*, 2007, **3**, 1996–2004.